Heat capacity and critical behavior of hexagonal $YMnO_3$

Makoto Tachibana, Junichiro Yamazaki, Hitoshi Kawaji, and Tooru Atake
Materials and Structures Laboratory, Tokyo Institute of Technology, 4259 Nagatsuta-cho, Midori-ku, Yokohama 226-8503, Japan
(Received 14 May 2005; published 16 August 2005)

We report heat capacity (C_p) measurements on high-quality single crystals of hexagonal $YMnO_3$, a ferroelectric and frustrated triangular antiferromagnetic (AF) compound. The obtained values of the critical exponent α and amplitude ratio A^+/A^- for the AF transition are in good agreement with the standard three-dimensional Heisenberg universality class, and not with a chiral universality class associated with the 120° spin structure. The low-temperature C_p deviation from the Debye law can be adequately fitted with a single Einstein contribution, indicating that there is no evidence of the anomalous magnetic contributions reported earlier. We also suggest that there is no intrinsic linear term in the low-temperature C_p. These results are consistent with conventional long-range AF ordering in $YMnO_3$.

DOI: 10.1103/PhysRevB.72.064434 PACS number(s): 75.50.Ee, 65.40.Ba, 75.40.Cx

I. INTRODUCTION

Recently, there has been a resurgence of significant interest in multiferroic materials, where ferroelectricity and magnetism coexist in a single compound. The coupling between these two order parameters is of fundamental interest, and may open routes for device applications. Among the various multiferroic materials reported recently, the rare-earth manganites show particularly interesting phenomena that are associated with the frustration of the Mn moments. In perovskite $R\mathrm{MnO_3}$ (R=Tb,Dy) (Ref. 1) and orthorhombic $R\mathrm{Mn_2O_5}$ (R=rare earth) (Ref. 2), the frustration of different Mn interactions is believed to be responsible for the magnetoelastically induced lattice modulations, which result in spontaneous polarization and ferroelectricity. As a direct consequence of the strong spin-lattice coupling, large magnetodielectric effects and electric polarization switching with the magnetic field are observed. In $R\mathrm{MnO_3}$ with the smaller rare-earth ions[3–5] (R=Ho—Lu,Y,Sc), the structure is hexagonal $P6_3cm$ with high ferroelectric Curie temperatures of ~1000 K. In this structure, the Mn^{3+} ions form triangular planar sublattices in the z=0 and 1/2 layers, which are stacked in the ABAB sequence along the z axis. For these systems, the geometrical frustration of antiferromagnetic (AF) spins on the triangular lattice results in the 120° spin ordering below the Néel temperature T_N of 70–130 K. Due to the large difference between the ferroelectric and spin-ordering temperatures, the coupling between the ferroelectricity and magnetism is expected to be small. However, for magnetic R^{3+}, the interactions between the ferroelectric polarization, the frustrated Mn^{3+} moments, and the magnetic moments on the R ions give rise to a complex magnetic phase diagram, whose stability can be controlled by an external electric field.[6]

In any case, the quasi-two-dimensional nature of the crystal structure[3] and the geometrical spin frustration of the triangular lattice are the sources of interesting magnetic behavior in hexagonal $R\mathrm{MnO_3}$. For $YMnO_3$ (T_N=75 K), previous neutron scattering studies[7,8] reported the presence of unconventional spin fluctuations both above and below T_N, which may be related to the anomalous increase in the thermal conductivity upon magnetic ordering.[9] These results were interpreted as evidence of strong geometrical frustration and/or low dimensionality, although it remains to be seen how the long-range order[10] can coexist with significant spin fluctuations in the Néel state for the triangular lattice. Perhaps even more surprising suggestions have been made in previous heat-capacity (C_p) studies[11,12] on $R\mathrm{MnO_3}$ (R=Y,Lu,Sc), where the large deviation of the low-temperature ($T<T_N$) C_p from the Debye law has been attributed to the residual magnetic contribution. This contribution is extremely large, and the broad shape of this anomaly implies that most of the spins are in a spin-glass-like state,[13] which is also inconsistent with the observation of 120° long-range spin structure. However, these studies have not considered the low-energy Einstein modes, the presence of which would significantly reduce the proposed magnetic contributions. Moreover, a significant linear term (~12 mJ K^{-2} mol^{-1}) in C_p for $YMnO_3$ was also reported,[14] which would indicate the presence of spin-glass contributions or unconventional magnetic excitations.

In addition to the unusual spin fluctuations, the questions regarding the symmetry of the order parameter and the nature of universality associated with the 120° spin structure have not been resolved. For triangular-lattice antiferromagnets with the 120° structure, the extra twofold degeneracy of chirality (corresponding to clockwise and counterclockwise spin arrangements) has been predicted to result in new universality classes for three-dimensional (3D) XY and Heisenberg models,[15] with $CsMnBr_3$ and VBr_2 being the respective examples.[16] For these chiral universality classes, large changes in the heat capacity critical exponent α and amplitude ratio A^+/A^- are reported, with the chiral XY and Heisenberg universality classes having α=0.34 and 0.24, compared to α=−0.01 and −0.12 for the standard XY and Heisenberg models, respectively (see Table I). As both α and A^+/A^- are significantly different between the chiral and standard classes, it is usually possible to distinguish these two classes with appropriate analysis. In a study employing single-crystalline $R\mathrm{MnO_3}$, Katsufuji *et al.*[11] have obtained α=0.25 from dielectric susceptibility measurements on $YMnO_3$, which is closer to the chiral than the standard universality

TABLE I. Critical exponent α and amplitude ratio A^+/A^- for various chiral and standard three-dimensional models (from Ref. 15), and the results for $YMnO_3$.

Model	α	A^+/A^-
Chiral *XY*	0.34(6)	0.36(20)
Chiral Heisenberg	0.24(8)	0.54(20)
Standard *XY*	−0.01	0.99
Standard Heisenberg	−0.12	1.36
$YMnO_3$	−0.16(1)	1.43(2)

classes. Moreover, they have obtained $\alpha=0.22$ for $T>T_N$ and $\alpha=0.10$ for $T<T_N$ from C_p measurements on $LuMnO_3$. While these values are also closer to the chiral universality classes, the different values for $T>T_N$ and $T<T_N$ are not consistent with the scaling prediction and may have arisen from the unconventional analysis employed in Ref. 11.

To elucidate the nature of magnetic ordering, we have performed C_p measurements on high-quality single crystals of $YMnO_3$. These measurements demonstrate that (i) the AF transition belongs to the standard 3D Heisenberg universality class, rather than a chiral universality class, (ii) the low-temperature ($T<T_N$) C_p is adequately fitted with lattice degrees of freedom, implying the absence of anomalous magnetic contributions, and (iii) the linear term is sample dependent and most likely of extrinsic origin, such as magnetic defects or impurities. Thus, these results provide a picture of rather conventional long-range spin ordering in $YMnO_3$.

II. EXPERIMENT

Single crystals of $YMnO_3$ were prepared by a flux method using Bi_2O_3 as the flux. $ScMnO_3$ crystals were also prepared with PbF_2 as the flux. For $YMnO_3$, both platelike and prismatic crystals were formed, with the latter belonging to the orthorhombic phase.[17] The powder x-ray diffraction patterns showed that the platelike crystals are of single phase with the hexagonal structure. Previous studies[18,19] have shown that neither Bi nor Pb incorporates into the crystals in detectable amounts. The C_p measurements were performed by a relaxation method using a Quantum Design PPMS.

III. RESULTS AND DISCUSSION

We show C_p of hexagonal $YMnO_3$ over the wide temperature range in the inset of Fig. 1, and in the vicinity of the AF transition in the main panel of Fig. 1. The data for two samples are plotted in the main panel, which show good agreement up to the immediate vicinity of the peak. For each sample, the data around the transition were taken from measurements on both the heating and cooling directions, and since the data display no thermal hysteresis effects, all the data are plotted together. Although the overall background C_p agrees well with previous studies, the transition is significantly sharper for the present samples and clearly shows signs of fluctuations.

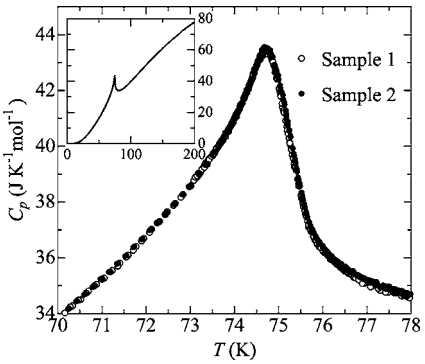

FIG. 1. Heat capacity of two samples of $YMnO_3$ in the vicinity of the antiferromagnetic transition. The inset shows the heat capacity in the wide temperature region.

Following the conventional critical analysis,[20] we have performed the least-squares fit of the data near the transition with $Cp^{\pm}=(A^{\pm}/\alpha)|t|^{-\alpha}+(B+Ct)$, where $t=(T-T_N)/T_N$. Here, $+$ and $-$ correspond to $t>0$ and $t<0$, respectively. In this form, $A^{\pm}$ are amplitude coefficients and $(B+Ct)$ includes both a physical smooth background and a constant offset. As usual, we assumed that $B^+=B^-=B$, i.e., there is no discontinuity at T_N. We find that the constraint $\alpha^+=\alpha^-=\alpha$, which is imposed by the scaling prediction, could be forced without significant sacrifice in the quality of the fit. In Fig. 2 we show C_p with the fit, where C_p is plotted vs t on a logarithmic scale. As expected, the data deviate from the fit in the close vicinity of T_N, and for the analysis, we have excluded the data in $|t|<5\times10^{-3}$ for $t<0$ and $|t|<10^{-2}$ for $t>0$. It should be noted that the manner of deviation from the fit is consistent with a Gaussian-distributed smearing of T_N,[21] which indicates that the rounding of the transition is associated with sample inhomogeneities. Above these regions, the α and A^+/A^- values obtained for sample 2 were stable with respect to the temperature region included in the fit. Moreover, multiplying a higher-order singular correction term $(1+D^{\pm}|t|^{0.5})$ to the power law did not improve the fit, indicating that the fit has been performed over the asymptotic critical regime. For sample 1, the fits were slightly poorer, and adding the correction term extended the stability of the fitting temperature region, but the obtained critical parameters were consistent with those of sample 2. In Fig. 2, the

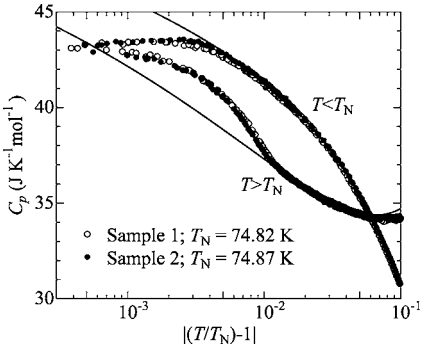

FIG. 2. Heat capacity of two samples of $YMnO_3$ vs reduced temperature in the logarithmic scale. The solid lines are the best fit to the data for sample 2, as described in the text.

solid lines show the best fit to the data for sample 2, with $\alpha=-0.16$ and $A^+/A^-=1.43$. Clearly, as seen in Table I, these values are very close to those expected for the standard 3D Heisenberg universality class, and far from both the *XY* and Heisenberg chiral universality classes, which have much larger α and lower A^+/A^- values.

The critical exponent α obtained in this study is significantly different from the various values reported in Ref. 11, which were obtained from dielectric susceptibility or heat-capacity measurements. However, given the evidence of spin-lattice coupling in $YMnO_3$,[9] the dielectric susceptibility may not provide a reliable value of α. Moreover, as discussed later, the lattice contribution estimated in Ref. 11 does not incorporate contributions from low-energy Einstein modes. The use of such a background for the critical analysis is known to provide erroneous values for α (Ref. 20), which is already evidenced by the different values for $T>T_N$ and $T<T_N$.[11]

For the 120° spin ordering in a triangular lattice, theories[15] predict that simultaneous ordering of the chirality results in a universality classes, and various examples of *XY* or Heisenberg chiral criticality have been reported in stacked triangular-lattice compounds.[16] Thus, the absence of chiral criticality in $YMnO_3$ suggests the removal of chiral degeneracy, which in turn implies the stabilization of a specific chirality on a given triangle. Katsufuji *et al.*[11] have suggested that the slight distortion of the ferroelectric lattice,[3] which is accompanied by the weak trimerization of the Mn ions,[11] may influence the critical behavior. On the other hand, although some modifications from the prototypical chiral behavior are expected for triangular AF systems with lattice distortions,[22] a single transition into the 120° structure with the standard criticality is not usually expected either.[16,22] In $RbMnBr_3$, the lattice distortion leads to an incommensurate spin structure with the spin angle slightly greater than 120°, but the chiral critical exponents are reported.[23] In $RbFeBr_3$ with the space group of $P6_3cm$, the lattice distortion leads to successive magnetic-phase transitions.

One possible mechanism for the chiral degeneracy removal is the symmetry breaking due to Dzyaloshinskii-Moriya (DM) interactions.[24] The antisymmetric DM exchange, which is specified by $\boldsymbol{D}(\boldsymbol{S}_1\times\boldsymbol{S}_2)$, is caused by the spin-orbit interactions and is sensitive to the structural distortions. Although such a mechanism has rarely been applied to triangular antiferromagnets,[26] DM interactions have been invoked[25] to explain the stability of different spin structures in kagomé-lattice compounds, where triangles are connected by the corners. For the kagomé lattice, the chirality is predicted to be determined by the sign of D_z, where the z axis is normal to the kagomé plane.[25] Although the kagomé lattice is different from a triangular lattice in that the chirality of the neighboring triangles can have the same sign (corresponding to the $\mathbf{q}=0$ structure),[25] similar arguments based on DM interactions should be able to explain how trimerized Mn ions in $YMnO_3$ stabilize a specific chirality, resulting in the chiral degeneracy removal. Also, it is interesting to note that DM interactions have been invoked to explain the coupling between ferroelectric and antiferromagnetic domain boundaries in $YMnO_3$,[27] as well as weak ferromagnetism[10] in $ScMnO_3$.[28]

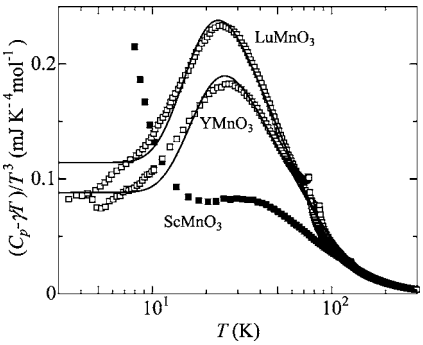

FIG. 3. Heat capacity divided by T^3 for $LuMnO_3$, $YMnO_3$, and $ScMnO_3$ vs T in the logarithmic scale. The data for $LuMnO_3$ are digitized from Ref. 11. For $LuMnO_3$ and $YMnO_3$, the linear contribution has been subtracted. For $ScMnO_3$, the raw data are shown. The solid lines are the fit to the Debye and Einstein functions, as described in the text.

Considering the quasi-two-dimensional nature of the crystal structure, the *XY* behavior may be expected over the Heisenberg behavior. However, the magnetic susceptibility[9] shows no sign of anisotropy for $T>T_N$, suggesting the Heisenberg nature of the interactions. The thermal-conductivity data are also more consistent with the isotropic spin interactions.[9] On the other hand, neutron-scattering measurements[7,8] showed the magnetic anisotropy to be $\sim 5-8\%$ of the predominant in-plane exchange interactions in $YMnO_3$. While these values are significant, they are more comparable to the values observed in the quasi-two-dimensional triangular BX_2 systems with the (chiral) Heisenberg criticality than those in the quasi-one-dimensional ABX_3 systems with the (chiral) *XY* criticality.[16]

We next consider the low-temperature ($T<T_N$) C_p of $R\mathrm{MnO}_3$ (R=Lu, Y, Sc), where the presence of unconventional spin fluctuations has been reported in neutron-scattering studies on $YMnO_3$.[7,8] In one study,[8] the spin fluctuations were correlated with the results of previous C_p studies,[11,12] where substantial amounts of residual magnetic contributions have been proposed. This proposal was based on the observation that C_p showed significant excess over the Debye function, which translates to a broad peak when C_p is plotted as C_p/T^3 (Ref. 11). In Fig. 3, we show the C_p/T^3 vs T plot of the present $YMnO_3$ and $ScMnO_3$ samples, and of $LuMnO_3$ taken from Ref. 11. As reported, a large broad peak is observed for $LuMnO_3$ and $YMnO_3$. However, it should be stressed that such a peak is usually associated with low-energy Einstein modes arising from a specific structural feature. In the layered $La_{2-x}Sr_xCuO_4$, for example, a peak in the C_p/T^3 plot at 23 K corresponds to an enhanced density of phonon states at 10 meV (Ref. 29), which is associated with the zone-boundary modes involving mostly La(Sr) ions.[30] As seen in Fig. 3, the peak becomes progressively larger in magnitude and is shifted down in temperature with the increasing mass of the *A*-site ion. This is consistent with the assumption that the peak is associated with the zone-boundary acoustic modes, as heavier *A* ions result in the flattening and downshift of this mode. To quantify this contribution, we have performed a fit with Debye and Einstein contributions, and the results are shown in Fig. 3 as solid lines.[31]

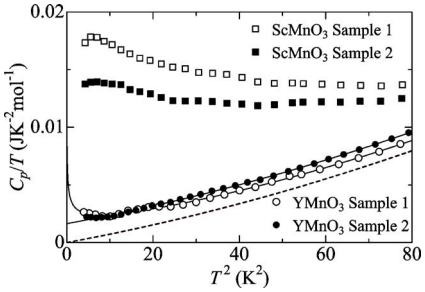

FIG. 4. The low-temperature heat capacity of two samples of $YMnO_3$ and $ScMnO_3$ plotted as C_p/T vs T^2. The solid lines are the best fits by $\gamma T^{\alpha}+\beta T^3+\beta_5 T^5$ (with $\alpha=0.37$ and 1.0 for samples 1 and 2, respectively). The dashed line represents the T^3 and T^5 terms of samples 1 and 2 of $YMnO_3$.

(In $YMnO_3$, an upturn at the lowest temperature region follows simple temperature dependence, as described later, and it was subtracted prior to the analysis. For $LuMnO_3$, a similar upturn follows linear temperature dependence with 1.0 mJ K^{-2} mol^{-1}, and was subtracted in Ref. 11.)

For $YMnO_3$, a Debye contribution with the temperature Θ_D of 425 K and the oscillator strength n_D of 10.5 per formula unit (f.u.) provides the constant contribution up to Θ_D, whereas an Einstein contribution with $\Theta_E=125$ K and $n_E=1.1$/f.u. provides the peak at 26 K in Fig. 3. For $LuMnO_3$, the best fit yields $\Theta_D=363$ K, $n_D=8.4$/f.u., $\Theta_E=115$ K, and $n_E=1.1$/f.u. Clearly, the larger peak observed at 24 K in $LuMnO_3$ is associated with the lower Debye and Einstein temperatures, which are consistent with the heavier Lu ions. For $ScMnO_3$, the upturn could not be subtracted reliably, but the much smaller peak at $\sim$30 K is consistent with the lighter Sc ions. These considerations lead us to conclude that there is no evidence of anomalous magnetic contributions in the heat capacity of $RMnO_3$. Accordingly, we view the shortfall of entropy under the peak at T_N (Ref. 11) to be mostly due to entropy already lost at higher temperatures, which is consistent with the evidence of short-range order at $T>T_N$ (Ref. 8).

Finally, we examine the nature of magnetic excitations in the lowest temperature region. This is motivated by the earlier observation of a large linear term with $\sim$12 mJ K^{-2} mol^{-1} in polycrystalline $YMnO_3$ (Ref. 14), which, for an insulating AF magnet, suggests the presence of a spin-glass contribution or unconventional magnetic excitations. In Fig. 4, we show the C_p data in C_p/T vs T^2 for several samples of $YMnO_3$ and $ScMnO_3$. The $ScMnO_3$ crystals show much larger C_p than the $YMnO_3$ crystals, showing an almost temperature-independent behavior with a broad peak below 3 K. The data extrapolate to $\sim$13–16 mJ K^{-2} mol^{-1}, which are similar in size to those observed for polycrystalline samples of $YMnO_3$ and $LuMnO_3$ (Ref. 14). Since the transition peak at T_N for the $ScMnO_3$ crystals was much broader than those observed for the $YMnO_3$ crystals but similar in shape to those of polycrystalline $YMnO_3$, the excess C_p observed in Fig. 4 is most naturally ascribed to magnetic defects or impurities.[32] On the other hand, the $YMnO_3$ crystals show much smaller C_p, but different temperature dependence is observed for the two samples. For sample 2, the data are best described by $\gamma T+\beta T^3+\beta_5 T^5$. The obtained linear term of $\gamma=1.6$ mJ K^{-2} mol^{-1} is much smaller than the value reported for the polycrystalline sample,[14] but is comparable to single-crystalline $LuMnO_3$ with 1.0 mJ K^{-2} mol^{-1} (Ref. 11). For sample 1, the linear term does not describe the data well, and the best fit is obtained by $\gamma T^{\alpha}+\beta T^3+\beta_5 T^5$, with $\alpha=0.37$ and $\gamma=3.6$ mJ K$^{-1.37}$ mol^{-1}.

The solid lines in Fig. 4 represent the best fit for each sample, which show a crossover at 3.5 K. However, when the subcubic terms are subtracted from these data, the two samples show indistinguishable T^3 and T^5 dependence, as represented by the dashed line. Thus, only the (quasi-) linear term is sample dependent on both the form and magnitude, which strongly suggests that it is an extrinsic contribution arising from magnetic defects or impurities. It should be noted that similar behavior was widely observed in high-T_c superconducting cuprates, where linear and sublinear contributions diminished with the improved sample quality.[33] As a final point, it should be noted that various forms of spin fluctuations observed in the neutron-scattering studies[7,8] are not inconsistent with the present C_p results, since they are either fast[7] (with the characteristic time scale of 55 ps) or diminish with decreasing temperature.[8] Our results are also consistent with spin-wave analysis of classical spins on the triangular lattice, which predicts conventional long-range order.[34]

IV. CONCLUSION

In conclusion, we have measured the heat capacity of $YMnO_3$ to examine the nature of its antiferromagnetic transition on the triangular lattice. The critical exponent α and the amplitude ratio A^+/A^- are consistent with the standard three-dimensional Heisenberg universality class. The absence of chiral criticality suggests the removal of chiral degeneracy, possibly due to Dzyaloshinskii-Moriya interactions. The low-temperature ($T<T_N$) deviation from the Debye law can be fully accounted for by a single Einstein contribution, indicating that there is no evidence of the anomalous magnetic contribution reported previously. We also find that the linear term in C_p is more naturally ascribed to extrinsic effects. These results provide a picture of conventional antiferromagnetic long-range ordering in $YMnO_3$.

ACKNOWLEDGMENTS

We thank H. Kawamura and H. Tanaka for valuable discussions, and Y. Kohama for assistance in data analysis. MT is supported by JSPS.

[1] T. Kimura, T. Goto, H. Shintani, K. Ishizaka, T. Arima, and Y. Tokura, Nature (London) **426**, 55 (2003); T. Kimura, S. Ishihara, H. Shintani, T. Arima, K. T. Takahashi, K. Ishizaka, and Y. Tokura, Phys. Rev. B **68**, 060403(R) (2003); T. Goto, T. Kimura, G. Lawes, A. P. Ramirez, and Y. Tokura, Phys. Rev. Lett. **92**, 257201 (2004).

[2] N. Hur, S. Park, P. A. Sharma, J. S. Ahn, S. Guha, and S.-W. Cheong, Nature (London) **429**, 392 (2004); L. C. Chapon, G. R. Blake, M. J. Gutmann, S. Park, N. Hur, P. G. Radaelli, and S.-W. Cheong, Phys. Rev. Lett. **93**, 177402 (2004).

[3] B. B. Van Aken, T. T. M. Palstra, A. Filippetti, and N. A. Spaldin, Nat. Mater. **3**, 164 (2004).

[4] M. Fiebig, T. Lottermoser, D. Frohlich, A. V. Goltsev, and R. V. Pisarev, Nature (London) **419**, 818 (2002).

[5] M. Fiebig, D. Fröhlich, K. Kohn, S. Leute, T. Lottermoser, V. V. Pavlov, and R. V. Pisarev, Phys. Rev. Lett. **84**, 5620 (2000).

[6] T. Lottermoser, T. Lonkai, U. Amann, D. Hohlwein, J. Ihringer, and M. Fiebig, Nature (London) **430**, 541 (2004).

[7] T. J. Sato, S.-H. Lee, T. Katsufuji, M. Masaki, S. Park, J. R. D. Copley, and H. Takagi, Phys. Rev. B **68**, 014432 (2003).

[8] J. Park, J.-G. Park, G. S. Jeon, H.-Y. Choi, C. Lee, W. Jo, R. Bewley, K. A. McEwen, and T. G. Perring, Phys. Rev. B **68**, 104426 (2003).

[9] P. A. Sharma, J. S. Ahn, N. Hur, S. Park, S. B. Kim, S. Lee, J.-G. Park, S. Guha, and S.-W. Cheong, Phys. Rev. Lett. **93**, 177202 (2004).

[10] A. Munoz, J. A. Alonso, M. J. Martinez-Lope, M. T. Casais, J. L. Martinez, and M. T. Fernandez-Diaz, Phys. Rev. B **62**, 9498 (2000).

[11] T. Katsufuji, S. Mori, M. Masaki, Y. Moritomo, N. Yamamoto, and H. Takagi, Phys. Rev. B **64**, 104419 (2001).

[12] D. G. Tomuta, S. Ramakrishnan, G. J. Nieuwenhuys, and J. A. Mydosh, J. Phys.: Condens. Matter **13**, 4543 (2001).

[13] K. Binder and A. P. Young, Rev. Mod. Phys. **58**, 801 (1986).

[14] T. Kyômen, M. Morita, M. Itoh, K. Kohn, and N. Kamegashira, Ferroelectrics **264**, 223 (2001).

[15] H. Kawamura, J. Phys.: Condens. Matter **10**, 4707 (1998).

[16] M. F. Collins and O. A. Petrenko, Can. J. Phys. **75**, 605 (1997).

[17] H. L. Yakel, W. C. Koehler, E. F. Bertaut, and E. F. Forrat, Acta Crystallogr. **16**, 957 (1963).

[18] S. H. Kim, S. H. Lee, T. H. Kim, T. Zyung, Y. H. Jeong, M. S. Jang, Cryst. Res. Technol. **35**, 19 (2000).

[19] J. E. Greedan, M. Bieringer, J. F. Britten, D. M. Giaquinta, and H.-C. zur Loye, J. Solid State Chem. **116**, 118 (1995).

[20] A. Kornblit and G. Ahlers, Phys. Rev. B **8**, 5163 (1973); **11**, 2678 (1975).

[21] H. v. Löhneysen, D. Beckmann, J. Wosnitza, D. Visser, J. Magn. Magn. Mater. **140-144**, 1469 (1995).

[22] H. Kawamura, Prog. Theor. Phys. Suppl. **101**, 545 (1990).

[23] An additional anomaly about 35 mK above the transition has been reported; F. Perez, T. Werner, J. Wosnitza, H. v. Löhneysen, and H. Tanaka, Phys. Rev. B **58**, 9316 (1998).

[24] I. Dzyaloshinskii, J. Phys. Chem. Solids **4**, 241 (1958); T. Moriya, Phys. Rev. **120**, 91 (1960).

[25] M. Elhajal, B. Canals, and C. Lacroix, Phys. Rev. B **66**, 014422 (2002).

[26] In $CsCuCl_3$, DM interactions are responsible for the spiral spin structure. However, the chiral criticality is observed up to the vicinity of the transition, where evidence of a crossover to a first-order transition has been reported; H. B. Weber, T. Werner, J. Wosnitza, H. v. Löhneysen, U. Schotte, Phys. Rev. B **54**, 15924 (1996).

[27] E. Hanamura, K. Hagita, and Y. Tanabe, J. Phys.: Condens. Matter **15**, L103 (2003).

[28] Weak ferromagnetism in $ScMnO_3$ has been questioned in M. Fiebig, D. Fröhlich, T. Lottermoser, and R. V. Pisarev, Phys. Rev. B **65**, 224421 (2002).

[29] A. P. Ramirez, B. Batlogg, G. Aeppli, R. J. Cava, E. Rietman, A. Goldman, and G. Shirane, Phys. Rev. B **35**, 8833 (1987).

[30] P. Böni, J. D. Axe, G. Shirane, R. J. Birgeneau, D. R. Gabbe, H. P. Jenssen, M. A. Kastner, C. J. Peters, P. J. Picone, and T. R. Thurston, Phys. Rev. B **38**, 185 (1988).

[31] Although a better fit can be obtained by increasing the number of modes employed in the analysis, our purpose here is to show that an adequate fit can be obtained with the simplest assumptions.

[32] This view is consistent with the reported magnetic susceptibility data, which show a large Curie upturn for polycrystalline samples (Refs. 10 and 12).

[33] J. S. Urbach, D. B. Mitzi, A. Kapitulnik, J. Y. T. Wei, and D. E. Morris, Phys. Rev. B **39**, 12391 (1989).

[34] T. Jolicoeur and J. C. Le Guillou, Phys. Rev. B **40**, 2727 (1989).